SWING-UP AND STABILIZATION OF FLEXIBLE UNDERACTUATED MANIPULATOR WITHOUT FEEDBACK

Hiroshi YABUNO *,1

* *Graduate School of Systems and Information Engineering, University of Tsukuba, Tsukuba, Ibaraki 305-8573, JAPAN*

Abstract: A control method without state feedback of the free link is proposed for swing-up and stabilization at the upright position of a flexible free link in a two-link underactuated flexible manipulator (the active first and free second links are rigid and flexible, respectively). The proposed method is based on the actuation of bifurcations produced in the second link under high-frequency excitation of the first link. Experimental results show the validity of the proposed method of control for the flexible underactuated manipulator.

Keywords: robotics, manipulator, high frequency, nonlinear control, pitchfork bifurcation, parametric resonance, perturbed bifurcation

1. INTRODUCTION

High-frequency periodic excitation realizes the stabilization of the unstable equilibrium states without feedback control (Kapitza, 1965) (Meerkov, 1980); this has been recognized in many fields for a considerably long time. In contrast with this phenomenon, high-frequency excitation can also destabilize stable equilibrium states (Schmitt and Bayly, 1998). These stabilization and destabilization phenomena under high-frequency excitation are produced through subcritical and supercritical pitchfork bifurcations, respectively.

In the previous study (Yabuno *et al.*, 2004), by utilizing the above pitchfork bifurcations under high-frequency excitation, a method of motion control for a two-link rigid underactuated manipulator, whose first link is connected to the first joint with only the actuator, without state feedback of the free link, is theoretically and experimentally proposed. In this study, we consider the method of control for an underactuated two-link manipulator with a flexible free link. The study of the flexible manipulator was first performed by Book et al. (Book *et al.*, 1975) and expanded by many researchers. However, for the 'flexible underactuated' manipulator, there are few reported control methods without feedback of the free link to our knowledge. There are, of course, many studies on 'rigid underactuated' manipulators, and comprehensive references can be found in (Arai *et al.*, 1998). In this study, similar to the previous control method for the rigid underactuated manipulator, the actuation of the bifurcations produced under high-frequency excitation for the active rigid first link is utilized for swinging the free link up to the upright position and stabilization in this state. Also, it is theoretically shown that the control method enables the above objectives to be accomplished independent of the elastic mode of the flexible free link, by setting the excitation frequency of the first link far from the natural frequencies of the elastic modes of the free link. Fur-

[1] Partially supported by the Japanese Ministry of Education, Culture, Sports, Science, and Technology, under Grant-in-Aid for Scientific Research 16560377.

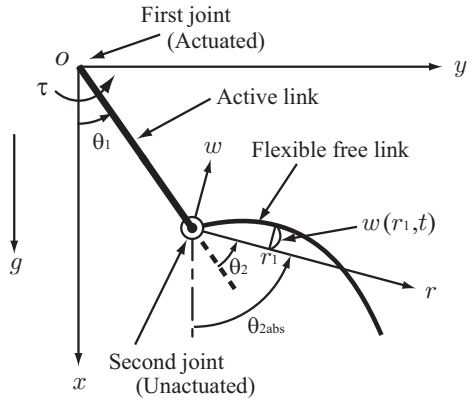

Fig. 1. Analytical model of flexible underactuated manipulator (the first link is a rigid body and the second link is an elastic body)

thermore, through experiments performed with an underactuated flexible manipulator, the effectiveness of the theoretically proposed control method is confirmed.

2. EQUATION OF MOTION OF FLEXIBLE UNDERACTUATED MANIPULATOR

The analytical model of a flexible underactuated manipulator is shown in Fig.1. The manipulator can be moved on the vertical plane. The active (first) joint has an actuator which can provide torque τ for the active (first) link. On the other hand, the flexible free (second) link cannot be controlled directly because the free (second) joint lacks not only an actuator but also a sensor. Under such conditions of the second joint, we cannot utilize state feedback, unlike in conventional studies on underactuated manipulators. Therefore, similar to the control method for the rigid free link proposed in the previous study (Yabuno *et al.*, 2004), we perform motion control of the flexible free link by using high-frequency excitation at the active joint. Hence, we set the angle of the first link as (it is easily realized in experiment by using commercial base position controller):

$$\theta_1 = a_{\theta 1} \cos \omega t + \theta_{1off}, \tag{1}$$

where the first term is a measure of the high-frequency excitation (hereafter, $a_{\theta 1}$ and ω are called the excitation amplitude and the excitation frequency, respectively). The second term θ_{1off} expresses the configuration of the first link with respect to the direction of gravity (hereafter, θ_{1off} is called "offset of excitation").

We introduce the axis r expressing the rigid mode of the flexible free link so as to satisfy

$$\int_0^{l_2} r \frac{\partial^2 w}{\partial t^2} w dr = 0, \tag{2}$$

where w is the elastic mode and l_2 is the length of the free link in the static equilibrium state. Also, assuming that the second link behaves like a Euler-Bernoulli beam, the x and y components of the absolute position of the second link at $r = r_1$ can be approximately expressed, under small elastic deflection w, as

$$\begin{aligned} x &= l_1 \cos\theta_1 + r_1 \cos\theta_{2abs} - w(r_1,t)\sin\theta_{2abs} \\ y &= l_1 \sin\theta_1 + r_1 \sin\theta_{2abs} + w(r_1,t)\cos\theta_{2abs}, \end{aligned} \tag{3}$$

where θ_{2abs} is the absolute angle of the rigid body mode of the free link expressed as:

$$\theta_{2abs} = \theta_1 + \theta_2. \tag{4}$$

Then, the kinetic energy T and the potential energy U can be shown as

$$\begin{aligned} T = {} & \frac{1}{2}(J + m_1 l_{1g}^2)\left(\frac{d\theta_1}{dt}\right)^2 \\ & + \frac{\rho}{2}\int_0^{l_2}\left\{ l_1^2\left(\frac{d\theta_1}{dt}\right)^2 + \left(\frac{\partial w}{\partial t}\right)^2 \right. \\ & + (r^2+\omega^2)\left(\frac{d\theta_{2abs}}{dt}\right)^2 + 2r\frac{\partial w}{\partial t}\frac{d\theta_{2abs}}{dt} \\ & \left. + 2l_1\frac{d\theta_1}{dt}\frac{d\theta_{2abs}}{dt}(r\cos\theta_2 - w\sin\theta_2)\right\} dr \end{aligned} \tag{5}$$

$$\begin{aligned} U = {} & -m_1 g l_{1g}\cos\theta_1 - \rho g \int_0^{l_2}\{l_1\cos\theta_1 \\ & + r\cos\theta_{2abs} - w\sin\theta_{2abs}\}\, dr \\ & + \frac{EI}{2}\int_0^{l_2}\left(\frac{\partial^2 w}{\partial r^2}\right)^2 dr, \end{aligned} \tag{6}$$

where m_1, l_1, l_{1g}, J, ρ, l_2, E, and I are the mass, length of the first link, the distance between the first joint and the center of gravity of the first link, the mass moment of inertia about the center of the first link, the linear density, the length of the second link, Young's modulus of elasticity, and the cross-sectional area moment. The values corresponding to the subsequent experimental apparatus are as follows: $m_1 = 0.0856\text{kg}, l_1 = 0.12\text{m}, l_{1g} = 0.051\text{m}, J = 3.9\times10^{-4} kg\cdot m^2, \rho = 4.3\times10^{-2}\text{kg/m}, l_2 = 0.174\text{m}, E = 12\times10^{10}\text{Ps}, I = 10.42\times10^{-13}$. The equations governing the behaviors of θ_1, θ_2, and w are obtained using Hamilton's principle. In the dimensionless form, the governing equations of the angle of the rigid-body mode and elastic modes of the second link, θ_2 and $w^* = w/l_2$, are expressed as

$$\begin{aligned} & \ddot{\theta}_{2bas} + c_1\dot{\theta}_1^2\sin\theta_2 + c_1\ddot{\theta}_1\cos\theta_2 + \sigma\sin\theta_{2abs} \\ & + \int_0^1 \{6\dot{w}^* w^* \dot{\theta}_{2abs} + 3w^{*2}\ddot{\theta}_{2abs} \end{aligned}$$

$$
\begin{aligned}
&-2c_1\dot{w}^*\dot{\theta}_1\sin\theta_2 - 2c_1 w\ddot{\theta}_1\sin\theta_2 \\
&+2c_1 w^*\dot{\theta}_1^2\cos\theta_2 + 2\sigma w^*\cos\theta_{2abs}\}dr \\
&+\mu_{\theta 2}\dot{\theta}_2 = 0 \qquad (7)
\end{aligned}
$$

$$
\begin{aligned}
&\ddot{w}^* + c_2 w^{*\prime\prime\prime\prime} - w^*\dot{\theta}_{2abs}^2 + r^*\ddot{\theta}_{2abs} \\
&+\frac{2}{3}c_1\dot{\theta}_1\dot{\theta}_{2abs}\sin\theta_2 + \frac{2}{3}\sigma\sin\theta_{2abs} + \mu_w\dot{w}^* = 0, \qquad (8)
\end{aligned}
$$

where $(\dot{})$ and $(')$ denote the partial derivatives with respect to dimensionless time $t^* = \omega t$ and dimensionless coordinate $r^* = r/l_2$, respectively, and the dimensionless parameters, c_1, c_2, and σ are expressed as $c_1 = 3l_1/(2l_2)$, $c_2 = EI/(\rho l_2^4\omega^2)$, $\sigma = 3g/(2l_2\omega^2)$.

In the above equations, viscous damping effects, $\mu_{\theta 2}\dot{\theta}_2$ and $\mu_w\dot{w}^*$ are also considered. The associated boundary conditions corresponds to those of the beam with hinged and free supported boundary conditions and are expressed as follows: $w^*|_{r^*=0} = w^{*\prime\prime}|_{r^*=0} = w^{*\prime\prime}|_{r^*=1} = w^{*\prime\prime\prime}|_{r^*=1} = 0$. Also, Eq. (1) is rewritten in the dimensionless form as

$$
\theta_1 = a_{\theta 1}\cos t^* + \theta_{1off} \qquad (9)
$$

Hereafter the asterisk is omitted.

3. THEORETICAL ANALYSIS

3.1 Modal expansion

First, we expand the elastic mode of the second link w by using the linear normal modes in

$$
\ddot{w} + c_2 w^{\prime\prime\prime\prime} = 0, \qquad (10)
$$

which corresponds to the equation obtained by neglecting the damping and nonlinear terms in Eq. (8). Using the before mentioned boundary conditions, w can be expanded with linear normal modes as follows:

$$
w(r,t) = \sum_{n=1}^{\infty} q_n(t)\cdot\varphi_n(r). \qquad (11)
$$

We substitute this equation into Eqs. (7) and (8), and account only for the first mode of w:

$$
w(r,t) \approx q_1(t)\cdot\varphi_1(r), \qquad (12)
$$

where $\varphi_1(r)$ is the first eigenmode, which is shown by using the first eigenvalue λ_1 as

$$
\varphi_1(r) = \sin\lambda_1 l_2\cdot\sinh\lambda_1 r + \sinh\lambda_1 l_2\cdot\sin\lambda_1 r.
$$

Then, the equations governing the dynamics of θ_2 and q_1 are written as

$$
\begin{aligned}
&(1+3\alpha_1 q_1^2)\ddot{\theta}_2 + (\mu_{\theta 2} + 6\alpha_1\dot{q}_1 q_1)\dot{\theta}_2 \\
&+(1 + c_1\cos\theta_2 + 3\alpha_1 q_1^2 - 2c_1\alpha_2 q_1\sin\theta_2)\ddot{\theta}_1 \\
&+c_1(\sin\theta_2 + 2\alpha_2 q_1\cos\theta_2)\dot{\theta}_1^2 + \sigma\sin\theta_{2abs} \\
&+(6\alpha_1 q_1 - 2\alpha_2 c_1\sin\theta_2)\dot{q}_1\dot{\theta}_1 \\
&+2\sigma\alpha_2 q_1\cos\theta_{2abs} = 0 \qquad (13)
\end{aligned}
$$

$$
\begin{aligned}
&\ddot{q}_1 + \mu_w\dot{q}_1 + (\omega_{w1}^2 - \dot{\theta}_{2abs}^2)q_1 - \dot{\theta}_{2abs}^2 q_1 + \beta_1\ddot{\theta}_{2abs} \\
&+\beta_2\dot{\theta}_1\dot{\theta}_{2abs}\sin\theta_2 + \beta_3\sigma\sin\theta_{2abs} = 0, \qquad (14)
\end{aligned}
$$

where $\alpha_n (n = 1, 2)$, ω_{w1}, and $\beta_n (n = 1, 2, 3)$ are dimensionless constant parameters which are governed by λ_1, φ_1, and l_2, respectively.

3.2 Bifurcation equation

In this section, by using the method of multiple scales (Nayfeh, 1973), we perform the averaging of Eqs. (13) and (14) in order to clarify the nonlinear characteristics of the bifurcation produced in the free link and to examine the dynamics of the elastic first mode of the free link. Before applying the analytical method, we perform the scaling of some parameters according to $c_2 = \epsilon^2\hat{c}_2, \sigma = \epsilon^2\hat{\sigma}, \mu_{\theta 2} = \epsilon\hat{\mu}_{\theta 2}, \mu_w = \epsilon\hat{\mu}_w$, and $a_{\theta 1} = \epsilon\hat{a}_{\theta 1}$, where $\hat{}$ denotes "of the order $O(1)$" and ϵ is a bookkeeping device. Then, using three time scales, we seek an approximate solution in the form

$$
\begin{aligned}
\theta_2 &= \theta_{20}(t_0,t_1,t_2) + \epsilon\theta_{21}(t_0,t_1,t_2) \\
&\quad + \epsilon^2\theta_{22}(t_0,t_1,t_2) + \cdots \qquad (15)
\end{aligned}
$$

$$
q_1 = \epsilon q_{11}(t_0,t_1) + \epsilon^2 q_{12}(t_0,t_1) + \cdots. \qquad (16)
$$

Substituting Eqs. (15) and (16) into Eqs. (13) and (14), considering Eqs. (4) and (9), and equating the coefficients of like powers of ϵ yield the following equations for the orders:

$O(\epsilon^0)$:

$$
D_0^2\theta_{20} = 0 \qquad (17)
$$

$O(\epsilon)$:

$$
D_0^2\theta_{21} = \hat{a}_{\theta 1}(1 + c_1\cos\theta_{20})\cos t_0 \qquad (18)
$$

$$
\begin{aligned}
&D_0^2 q_{11} + \left\{\omega_{w1}^2 q_{11} - (D_0\theta_{20})^2\right\} q_{11} = \beta_1 D_0^2\theta_{21} \\
&-2\beta_1 D_0 D_1\theta_{20} - \beta_1\hat{a}_{\theta 1}(1 + c_1\cos\theta_{20})\cos t_0 \\
&+\beta_2\hat{a}_{\theta 1}D_0\theta_{20}\sin t_0\sin\theta_{20} \qquad (19)
\end{aligned}
$$

$O(\epsilon^2)$:

$$
\begin{aligned}
&D_0^2\theta_{22} = -D_1^2\theta_{20} - \hat{\mu}_{\theta 2}D_1\theta_{20} \\
&-\frac{\hat{a}_{\theta 1}^2 c_1^2}{2}(1+\cos 2t_0)\sin\theta_{20}\cos\theta_{20} \\
&-\hat{a}_{\theta 1}c_1\theta_{21}\cos t_0\sin\theta_{20} \\
&-\hat{\sigma}\sin(\theta_{1off} + \theta_{20}) + \cdots \qquad (20)
\end{aligned}
$$

$$
\begin{aligned}
&D_0^2 q_{12} + \left\{\omega_{w1}^2 - (D_0\theta_{20})^2\right\} q_{12} = -2D_0 D_1 q_{11} \\
&-\hat{\mu}_w D_0 q_{11} + \ldots \qquad (21)
\end{aligned}
$$

Here, $D_i = \partial/\partial t_i$. First, from Eq. (17), we obtain the general solution of θ_{20} as

$$\theta_{20} = C_1 t_0 + C_0(t_1, t_2). \tag{22}$$

We set the integral constant of C_1 to zero to eliminate the secular term in Eq. (22). Considering that θ_{20} is not a function of t_0, we obtain

$$D_0^2\theta_{21} = \hat{a}_{\theta 1}(1 + c_1\cos\theta_{20})\cos t_0 \tag{23}$$

$$D_0^2 q_{11} + \omega_{w1}^2 q_{11} = \beta_1\hat{a}_{\theta 1}(1 - c_1\cos\theta_{20})\cos t_0. \tag{24}$$

The particular solution of Eq. (23) and the general solution of Eq. (24) become

$$\theta_{21} = -\hat{a}_{\theta 1}(1 + c_1\cos\theta_{20})\cos t_0 \tag{25}$$

$$q_{11} = a_{w1}(t_1)\cos\{\omega_{w1}t_0 - \gamma_{w1}(t_1)\} - \frac{\beta_1\hat{a}_{\theta 1}c_1\cos\theta_{20}}{\omega_{w1}^2 - 1}\cos t_0. \tag{26}$$

Furthermore, substituting Eqs. (25) and (26) into Eqs. (20) and (21) and considering that θ_{20} is not a function of t_0, the conditions for the elimination of secular terms from θ_{22} and q_{12} are expressed as

$$D_1^2\theta_{20} + \hat{\mu}_{\theta 2}D_1\theta_{20} - \frac{\hat{a}_{\theta 1}^2 c_1^2}{2}\sin\theta_{20}\cos\theta_{20} + \hat{\sigma}\sin(\theta_{20} + \theta_{1off}) = 0 \tag{27}$$

$$D_1 a_{w1} = -\frac{\hat{\mu}_{w1}}{2}a_{w1}, D_1\gamma_{w1} = 0. \tag{28}$$

From Eq. (28), the amplitude of the homogenous solution in the first elastic mode of the free link a_{w1} decays as follow:

$$a_{w1} = a_{w10}\mathrm{e}^{-\hat{\mu}_{w1}t_1/2} = a_{w10}\mathrm{e}^{-\mu_{w1}t/2}, \tag{29}$$

where a_{w10} is a constant determined from the initial condition. If the excitation frequency of the first link (the dimensionless excitation frequency is 1) is not in the neighborhood of the first natural frequency of the elastic mode of the free link ω_{w1}, the amplitude of the oscillation of the elastic mode does not increase and remains in the order of $O(\epsilon)$. Similarly, for any other higher modes, it can be theoretically predicted that the magnitudes do not increase with time. Therefore, we can neglect the elastic mode and focus on the rigid body mode θ_2 for the proposition of motion control of the free link.

Multiplying both sides of Eq. (27) by ϵ^2 yields the approximate equation governing the dynamics of the rigid-body mode of the free link, as follows:

$$\ddot{\theta}_{20} + \mu_{\theta 2}\dot{\theta}_{20} - \frac{a_{\theta 1}^2 c_1^2}{2}\sin\theta_{20}\cos\theta_{20} + \sigma\sin(\theta_{20} + \theta_{1off}) = 0. \tag{30}$$

Because this equation is autonomous, neglecting $\ddot{\theta}_{20}$ and $\dot{\theta}_{20}$ leads to a bifurcation equation similar to that in the case when the free link is rigid (Yabuno *et al.*, 2004).

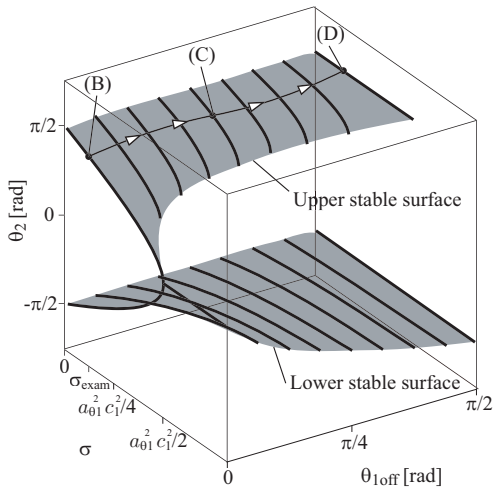

Fig. 2. Equilibrium surface (the combinations of θ_2, θ_{1off}, and σ corresponding to any points on the equilibrium surface show stable configurations of the manipulator)

4. BIFURCATION PHENOMENA PRODUCED IN THE FREE LINK

By changing θ_{1off} (the direction of the gravity effect) and σ (proportional to $1/\omega^2$), the equilibrium points are varied continuously. Let us set the excitation frequency of the first joint to values that are not in the neighborhood of the natural frequency of the first elastic mode. Then, similar to that in the previous paper, it is shown that under sufficiently constant high-frequency excitations, i.e., $\sigma < a_{\theta 1}^2 c_1^2/4$ and the change of the offset of excitation θ_{1off} from 0 to $\pi/2$ swing-up and stabilization at the upright position are accomplished without state feedback of the free joint.

By obtaining equilibrium points and examining their stabilities by using Eq. (30), we can show the regions in the equilibrium surface which consist of the stable equilibrium points as hatched surfaces in Fig. 2; hereafter we call these hatched surfaces stable equilibrium surfaces or stable surfaces for short. The points on the surface, such as (B), (C), and (D), are discussed in the next section. This figure shows the sets of all stable equilibrium points produced through the pitchfork bifurcations under high-frequency excitation, i.e., small σ, and through their perturbations under the change in the offset of excitation, i.e., actuation of θ_{1off}. The cross sections of the stable equilibrium surface in Fig. 2 and the planes $\theta_{1off} = 0$, $\theta_{1off} = \pi/4$, and $\theta_{1off} = \pi/2$ correspond to the stable equilibrium branches in the bifurcation diagrams of Figs. 3, 4, and 5, which are obtained from Eq. (30) under the conditions $\theta_{1off} = 0$, $\theta_{1off} = \pi/4$, and $\theta_{1off} = \pi/2$, respectively. The left and right ordinates are the relative and absolute angles of the free link, respectively.

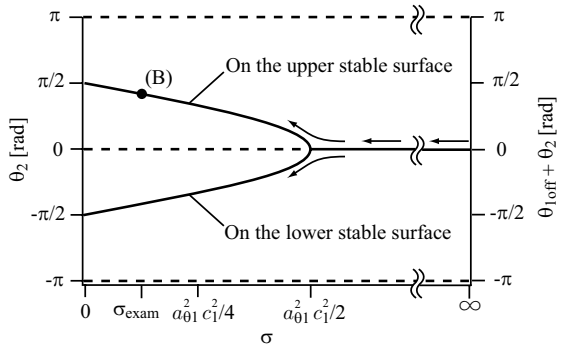

Fig. 3. Bifurcation phenomena in the free link in the case of $\theta_{1off} = 0$ (supercritical pitchfork bifurcation occurs at $\sigma = a_{\theta 1}^2 c_1^2/2$)

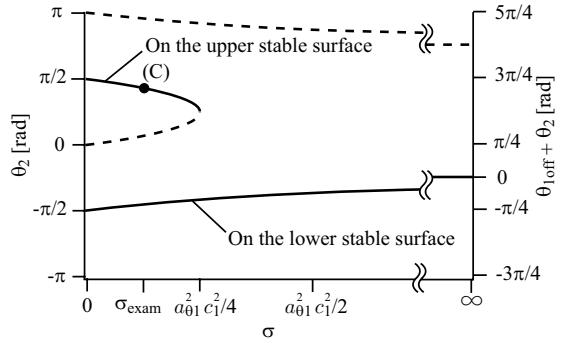

Fig. 4. Bifurcation phenomena in the free link in the case of $\theta_{1off} = \pi/4$ (perturbed supercritical and subcritical pitchfork bifurcations occur at $\sigma = a_{\theta 1}^2 c_1^2/4$)

In the case of $\theta_{1off} = 0$, a supercritical pitchfork bifurcation is produced at $\sigma = a_{\theta 1}^2 c_1^2/2$, as shown in Fig. 3. In the case of $\sigma < a_{\theta 1}^2 c_1^2/2$, i.e., when the excitation frequency is sufficiently high, the equilibrium state $\theta_2 = 0$, where the second link hangs down in the direction of gravity, is changed to be unstable and simultaneously, the nontrivial stable equilibrium state is produced. Then, the second link is swung up from the direction of gravity. When we increase the offset of excitation, various perturbations of the bifurcation are produced. For example, in the case of $\theta_{1off} = \pi/4$, the supercritical pitchfork bifurcation is perturbed (the combination of the lower three equilibrium states), as in Fig. 4, and the combination of the upper three equilibrium states is also regarded as a perturbed subcritical pitchfork bifurcation. Furthermore, we increase the offset of excitation, and when θ_{1off} is $\pi/2$, a subcritical pitchfork bifurcation is produced at $\sigma = a_{\theta 1}^2 c_1^2/2$, as shown in Fig. 5. In the case of $\sigma < a_{\theta 1}^2 c_1^2/2$, i.e., when the excitation frequency is sufficiently high, the equilibrium state $\theta_2 = \pi/2$ ($\theta_{1off} + \theta_2 = \pi$), where the second link is in the upright position, is stable.

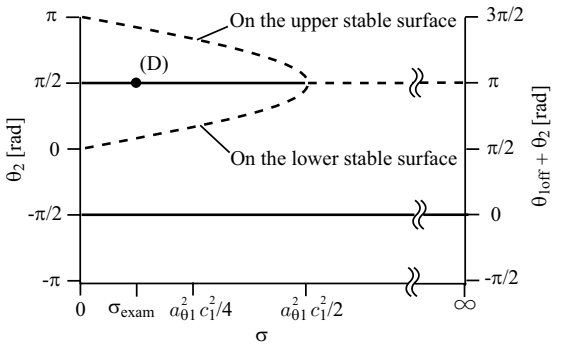

Fig. 5. Bifurcation phenomena in the free link in the case of $\theta_{1off} = \pi/2$ (subcritical pitchfork bifurcation occurs at $\sigma = a_{\theta 1}^2 c_1^2/2$)

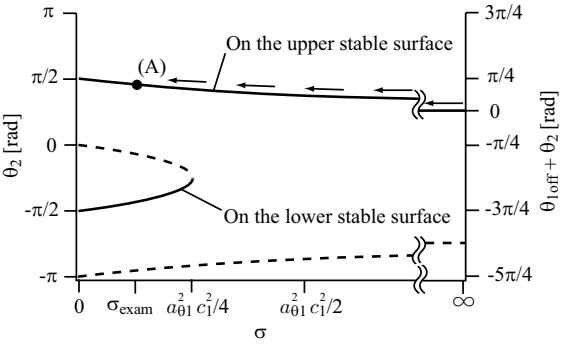

Fig. 6. Bifurcation phenomena in the free link in the case of $\theta_{1off} = -\pi/4$ (perturbed supercritical and subcritical pitchfork bifurcations occur at $\sigma = a_{\theta 1}^2 c_1^2/4$)

5. MOTION CONTROL WITHOUT STATE FEEDBACK

5.1 Control strategy by actuating the bifurcations

From the above results, it is seen that the change of the offset of excitation θ_{1off} realizes the actuation of the bifurcations, i.e., many types of bifurcation phenomena can be produced. By continuously changing the offset of excitation, it is possible to move the stable equilibrium states of the free link. Now, let us consider the swing-up of the free link and the stabilization at the upright position. For example, we set the excitation frequency to ω_{exam}, i.e., the parameter σ to $\sigma_{exam} = 3g/(2l_2\omega_{exam}^2)$ (see Fig. 2). Because the initial offset of the excitation is $\theta_{1off} = 0$, the state of the free link can be located at (B) on the equilibrium surface in Fig. 2 under the excitation frequency. Then, by changing the offset of excitation θ_{1off}, the stable equilibrium state is moved from point (B) to (D) on the equilibrium surface and swing-up is accomplished. These points correspond to those in Figs. 3, 4, and 5, respectively. Furthermore, it is noted from the bifurcation diagram of Fig. 5 that the upright position, i.e., point (D), is stable.

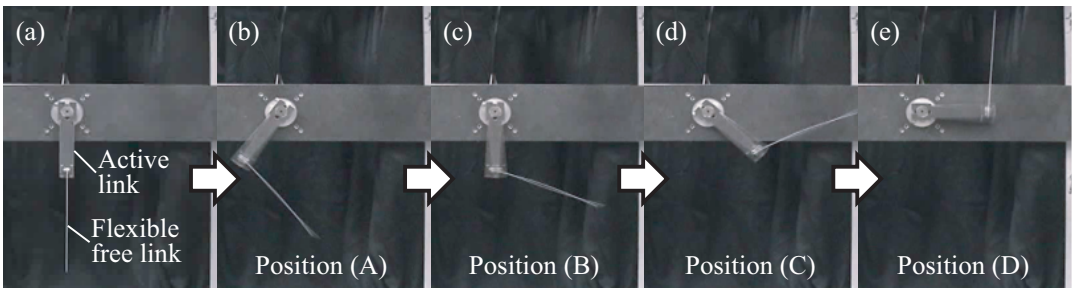

Fig. 7. Experiment of underactuated manipulator (swing-up of the flexible free link and stabilization at the upright position)

When we increase the excitation frequency ω from 0 to ω_{exam}, i.e., decrease σ from $+\infty$ to σ_{exam}, at the first stage of control ($\theta_{1off} = 0$), the probability that the free link can be put on the upper or lower branch in the bifurcation diagram, Fig. 3, i.e., on the upper stable surface or the lower stable one in Fig. 2, is 50% because the bifurcation is completely supercritical, as indicated by the arrow in Fig. 3. To definitely put the state on upper surface, we set θ_{1off} to be negative (for example, $\theta_{1off} = -\pi/4$). Then the bifurcation diagram is expressed as in Fig. 6. In this case, the state of the free link moves along the arrows in Fig. 6 with increasing excitation frequency and can definitely be put on the upper branch. After that, by changing θ_{1off} to $\pi/2$ continuously, swing-up is accomplished following the arrows in Fig. 2 ($(A) \rightarrow (B) \rightarrow (C) \rightarrow (D)$).

5.2 Experiment

We experimentally confirm the validity of the theoretically proposed control method. The active (first) link is actuated by an AC servomotor with a rotary encoder (Mitsubishi Corp., HC-MFS73 (maximum torque: 7.2 Nm, rated output: 750 W)). The flexible free (second) link does not have an actuator or a sensor. A CCD camera (Sony Corp., XC-77) is used for recording the behavior of the manipulator under motion control; this data is not used in motion control. We show an experimental result of swing-up of the flexible free link indicated by changing the offset of excitation of the active link. Fig. 7 (a) shows the static equilibrium position ($a_{\theta 1} = \omega = \theta_{1off} = 0$). The configurations of the manipulator, (B), (C), and (D) in Figs. 7 (c), (d), and (e), correspond to the points (B), (C), and (D) in Figs. 3, 4, and 5, respectively. Here, the excitation frequency of the active link is constant at 45 Hz in motion control from Figs. 7 (b) to (e). Swing-up of the free link is accomplished without state feedback of the free link when the offset of excitation reaches $\theta_{1off} = \pi/2$. Also, the upright position of the free link is stable without state feedback of the free link.

6. CONCLUSION

In this study, a method of motion control without state feedback of the flexible free link is proposed for a two-link flexible underactuated manipulator, in which the first (active) link is rigid and the second (free) link is flexible, wherein the pitchfork bifurcation is induced under the high-frequency excitation and the perturbation of the bifurcation is actuated. The control method can be regarded as that of manipulators in the case when not only the actuator but also the sensor breaks down. Experimental results for an underactuated flexible manipulator confirm the validity of the proposed motion control method.

REFERENCES

Arai, H., K. Tanie and N. Shiroma (1998). Nonholonomic control of a three-dof planar underactuated manipulator. *IEEE Trans. Robot. Automat.* **14**, 681–695.

Book, W.J., O. Maizza-Neto and D.E. Whitney (1975). Feedback control of two beam, two joint systems with distributed flexibility. *Trans. ASME, J. Dyn. Syst. Meas. Control* **97**, 424–431.

Kapitza, P.L. (1965). Dynamical stability of a pendulum when its point of suspension vibrates, and pendulum with a vibrating suspension. In: *Collected papers of K.L. Kapitza* (D.T. Haar, Ed.). 1st ed.. Vol. 2. pp. 714–737. Pergamon Press. London.

Meerkov, S.M. (1980). Principle of vibrational control: theory and applications. *IEEE Trans. Auto. Contr.* **25**, 755–762.

Nayfeh, A.H. (1973). *Perturbation method.* John Wiley & Sons. New York.

Schmitt, J.M. and P.V. Bayly (1998). Bifurcations in the mean angle of horizontally shaken pendulum: analysis and experiment. *Nonlinear Dynamics* **15**, 1–14.

Yabuno, H., K. Goto and N. Aoshima (2004). Swing-up and stabilization of an underactuated manipulator without state feedback of free joint. *IEEE Trans. Robot. Automat.* **20**, 399–365.